

PixelArena: A benchmark for Pixel-Precision Visual Intelligence

Feng Liang* Sizhe Cheng* Chenqi Yi

Nanyang Technological University
50 Nanyang Avenue, Singapore

{feng011, sizhe003, chenqi001}@e.ntu.edu.sg

Abstract

Multi-modal large language models that have image output are emerging. Many image generation benchmarks focus on aesthetics instead of fine-grained generation capabilities. In PixelArena, we propose using semantic segmentation tasks to objectively examine their fine-grained generative intelligence with pixel precision. We find the latest Gemini 3 Pro Image has emergent image generation capabilities that generate semantic masks with high fidelity under zero-shot settings, showcasing visual intelligence unseen before and true generalization in new image generation tasks. We further investigate its results, compare them qualitatively and quantitatively with those of other models, and present failure cases. The findings not only signal exciting progress in the field but also provide insights into future research related to multimodality, reasoning, interpretability and benchmarking.

1. Introduction

Since the release of GPT-4o [25] in 2024, multi-modal large language models (MLLMs), which have multiple output modalities (*e.g.*, text, images, and audio), have been a focus of research. Numerous models have been developed (*e.g.*, Emu series [7, 29–31], Gemini series [8, 9]). They can generate images based on prompts that include both text and images. This capability is highly malleable, enabling flexible in-context learning and powerful, convenient, and conversational image generation. However, as much focus has been placed on image quality and aesthetics, few have quantitatively examined the precision and generalizability of the image generation capabilities of these models, nor have they examined the limitations of visual reasoning and perception of these models during image generation.

In PixelArena, we propose using pixel-level tasks (*e.g.*, face parsing and general semantic segmentation) to examine MLLMs’ fine-grained control capability and their gen-

eralizability in image generation, which we term pixel-precision visual intelligence (PPVI). Specifically, we ask models to perform semantic segmentation (*e.g.*, face parsing) with the CelebAMask-HQ [17] and COCO [21] datasets. This allows us to use objective metrics to measure fine-grained generative capability in terms of precision. Qualitatively and quantitatively, we found that Gemini 3 Pro Image [9] represents a significant leap in this front by comparing the results from previous models. With quantitative results, we also show that Gemini 3 Pro Image truly generalizes to new image generation tasks. We also present interesting failure cases and analyze their implications.

In summary, our contributions are:

1. We propose PixelArena, in which pixel-level tasks (*e.g.*, semantic segmentation) are used to quantitatively measure MLLMs’ fine-grained control capability and their generalizability (*i.e.*, PPVI) in image generation tasks.
2. We task MLLMs to perform face parsing with the CelebAMask-HQ [17] dataset, revealing surprising emergent zero-shot capabilities in Gemini 3 Pro Image [9]. We also performed experiments to examine potential data contamination in this model, showing that the model did not memorize the answers (*i.e.*, reference masks) but truly understood this image generation task.
3. We present the results of semantic segmentation on a more challenging dataset, COCO [21], showing that Gemini 3 Pro Image still has reasonable performance and generalization.
4. We have conducted qualitative and quantitative analyzes of the results, including failure cases, hinting at more future directions in multi-modality, reasoning, and interpretability research.

Our website for inspecting the results of PixelArena is available at <https://pixelarena.reify.ing>.

*These authors contributed equally to this work.

2. Related Work

2.1. Semantic Segmentation and Face Parsing

In computer vision research, many segmentation datasets have been developed, such as COCO [21], a large-scale benchmark containing object-centric images with pixel-level annotations for diverse everyday scenes; FSS-1000 [19], a few-shot segmentation dataset featuring 1,000 object categories with only a single annotated example per class; SA-CO [4], which extends segment-anything-style annotation to concept-driven segmentation tasks; and SA-MED2D [32], a medical-domain dataset designed to evaluate generalizable 2D segmentation across varied clinical imagery.

We use face parsing with the CelebAMask-HQ [17] dataset as an example, a high-quality facial image dataset that provides detailed pixel-level annotations for 18 distinct facial components across 30,000 celebrity images. Various models have been proposed to push the state of the art on CelebAMask-HQ. The general facial representation model FaRL [36] achieves strong face parsing performance by leveraging large-scale vision-language pretraining and transferring it to CelebAMask-HQ. SegFace [24] improves the state of the art on CelebAMask-HQ by explicitly addressing long-tail facial components through a balanced segmentation framework.

Another example we present is general semantic segmentation on the panoptic segmentation dataset of the COCO [21] dataset. OneFormer [13] and Mask2Former [6] are the state-of-the-art models on this dataset. They are capable of performing universal image segmentation (*i.e.*, semantic segmentation, instance segmentation, and panoptic segmentation) with a single model.

Note that in PixelArena, we do not intend to use MLLMs to compete with these specialized models; instead, we probe the emergent capabilities and generalizability of these generalist models. In our experiments, we task MLLMs to generate masks with published weights or public APIs and no further training.

2.2. Image Generation Benchmarks and Metrics

Most of the benchmarks [10–12, 14, 16, 18, 27, 28, 33–35] for text-to-image generation and image editing focus on evaluating generated natural images rather than the masks that we use. However, due to their diversity and complexity, natural images are difficult to evaluate, and the evaluation metrics are often subject to implicit human preferences or model biases. For example, in HEIM [18], the metrics used are CLIP score, FID, the score from a LAION aesthetics predictor, human evaluation score, and VQA-based scores. However, the CLIP score, FID, aesthetics score and VQA-based scores may be biased by the models used, while human evaluation is fundamentally based on implicit preferences.

These metrics are fundamentally subjective.

In PixelArena, because we task models to generate masks and evaluate the generated masks, we can use standard objective metrics like F1 Score and mIoU.

2.3. Segmentation with MLLMs

Previous research focuses on integrating a MLLM that has multi-modal input but *text-only output* with a segmentation model. For example, RAS [2] enhances segmentation models by integrating a mask-centric large multimodal model that selects relevant mask groups from a pool of candidates based on vision-language prompts, enabling flexible and precise mask grouping. SAM4MLLM [5] trains a MLLM to output prompts (bounding boxes and points) to guide SAM [15] in generating accurate segmentation masks, thus combining language understanding with pixel-level mask generation. In SAM 3 [4], the authors propose SAM Agent, which is similar to SAM4MLLM [5]. The large multimodal model for remote sensing images [22] uses a language model to interpret open-vocabulary queries and conditions a segmentation decoder to produce class-specific masks, enabling flexible, high-resolution semantic segmentation of unseen categories. All of them integrate a MLLM and a segmentation model with text or latent vectors as intermediate representations. However, in PixelArena, we use the original MLLMs *without* any tools, model extensions, or finetuning. Noteworthy is that in SAM 3, the researcher presented preliminary results generated by Gemini 2.5 Flash Image in object detection tasks with ODinW13 [3] and RF-100VL [26] using prompts and few-shot learning. These results are closely related to ours, but their output is bounding box coordinates, while ours are mask images. We test the finer-grained capabilities of MLLMs at the pixel level with image generation.

3. Methods

3.1. Dataset

We use subsets of the COCO [21] and CelebAMask-HQ [17] datasets as examples.

For the CelebAMask-HQ [17] dataset, we randomly sampled 150 images and their corresponding masks. As the reference masks are 512×512 , while the selected MLLMs [7–9, 20, 25] natively support image generation with resolutions larger than 512×512 (*e.g.*, 720×720 and 1024×1024), we upsampled the reference masks using nearest neighbors to 1024×1024 . We also upsampled the generated masks using nearest neighbors to 1024×1024 .

For the COCO [21] dataset, we randomly sampled 150 images and their corresponding masks from its panoptic segmentation dataset. We convert the panoptic masks into semantic segmentation masks using its official toolkit¹. As

¹<https://github.com/cocodataset/panopticapi>

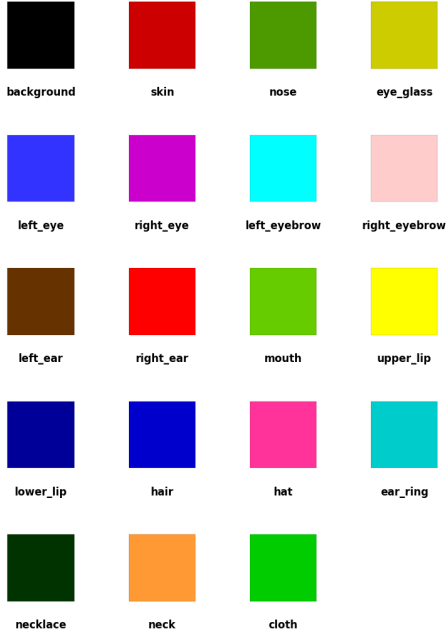


Figure 1. Palette of the standard color encodings from CelebAMask-HQ [17]

the resolutions of the images and masks in the dataset are not fixed, we center-crop them based on the shortest dimensions to obtain square ones. Similarly, we upsample the reference masks and generated masks to 1024×1024 using nearest neighbors.

In the following sections, we refer these two subsets as the `celeb` and `coco` datasets, respectively. Unless specified otherwise, we evaluate the metrics (*i.e.*, F1 Score, mIoU, and Dice) with upsampled masks.

3.2. Models and Mask Generation

With different models, we use various methods to generate valid masks.

For MLLMs: We select recent models with strong image generation capabilities, including Gemini 3 Pro Image (gmn3) [9], Gemini 2.5 Flash Image (gmn25) [8], GPT Image 1 (gpti) [25], Emu 3.5 (emu35) [7], and Uni-MoE-2 (unimoe2) [20]. Note that we tested two variants of unimoe2, Uni-MoE-2 Omni (unimoe2-omni) the flagship model of the series, and Uni-MoE-2 Image (unimoe2-image) the variant finetuned for image generation. For the sake of brevity, we will refer to them by their short code names in the following sections.

As they natively generate images instead of label vectors, we first prompt them to generate images and then convert the pixels from RGB values to class labels. The prompts for the two datasets are composed of three parts: an image from the dataset, an image of the color palette of label encodings

(Fig. 1 and 13), and a short text (Listing 1 and 2 in Supplementary). These prompts provide task specifications and visual grounding for the color encodings, as well as some clarifications. Note that no examples are given, meaning the models have to learn face parsing and general semantic segmentation *zero shot*. For the sampling parameters of the MLLMs, refer to Table 1 in Supplementary.

Given the mask images from MLLMs, we compare the RGB value of each pixel with the color encodings for the labels, selecting the nearest color and label. It is formulated as Eq. 1, where \vec{e}_i is the RGB color vector of label i , and \vec{p} is the color vector of a pixel.

$$\text{Label Index } i = \operatorname{argmin}_i (\vec{e}_i \cdot \vec{p}) \quad (1)$$

For SAM 3: SAM 3 (sam3) [4] accepts text as the prompt for mask generation. We prompt `sam3` with the labels of CelebAMask-HQ [17] one by one and merge the corresponding 19 masks into one final mask. For the label of each pixel in the overlapping areas of these masks, we randomly pick one from the overlapping labels.

For specialized computer vision models: We use the pretrained ConvNext [23] variant of SegFace (segface) [24] as a strong baseline model on `celeb`. On `coco`, we use OneFormer (1former) [13] as a strong baseline model.

4. Analysis

Due to the stochastic components (*e.g.*, token sampling, diffusion module) in MLLMs, the generation of mask images is inherently stochastic. Therefore, we present results from multiple attempts (*i.e.*, $p = [1, 3, 5]$).

4.1. Qualitative Comparisons

In Fig. 2, we present results of different models on `celeb` for qualitative comparison. Among all MLLMs, gmn3 is the *only* one that understands the task requirements *and* completes it with high quality. gpti and gmn25 partially understand the task, but gmn25 lacks precise color control or fails to understand the color encodings, while gpti lacks precise control over the composition of the image, hallucinating the upper body of the person. As for sam3, it sometimes misses some labels. emu35 and unimoe2 models completely misunderstood the task while they present different failure patterns. emu35 failed to draw plausible masks but we can see that it could control its image generation process to replicate most features in the original image. In contrast, unimoe2 models could not even draw an image similar to the original image, which may be due to its vision system failing to capture the original image, failing to propagate the visual information to its generation module, or failing to control its generation process.

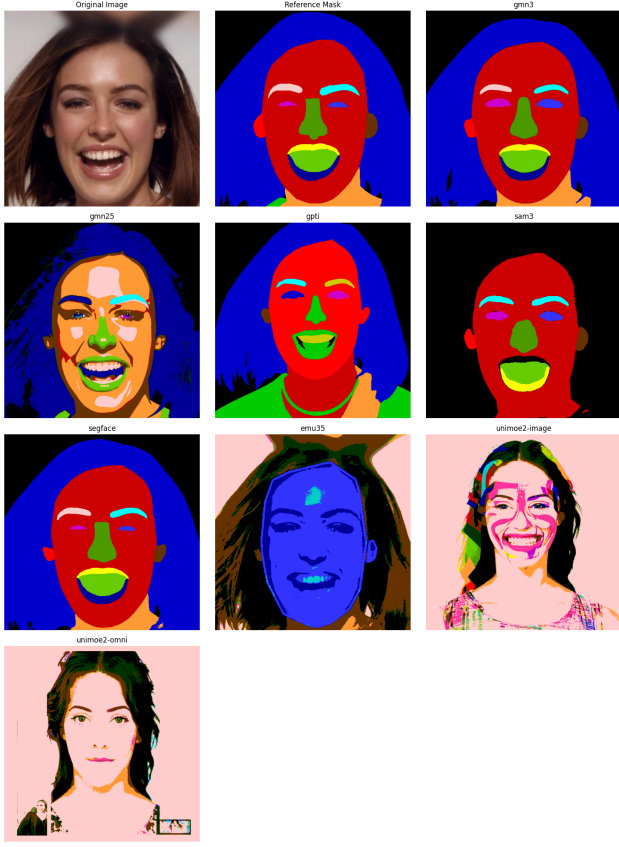


Figure 2. Comparison between the Results of Different Models on celeb. Not cherrypicked.

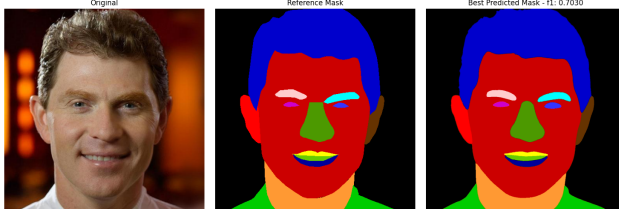


Figure 3. Best prediction across celeb by gmn3 with F1 score 0.7030.

Such failure modes are common in the results of the respective models, implying potential misalignment between the vision system and the generation module or lack of control over the generation process.

We further investigate the results of gmn3. We present the best and worst results from the model in Fig. 3 and Fig. 4. The best prediction has a nearly indistinguishable difference from the reference mask, while the worst prediction is dramatically low in quality. However, the other two attempts in Fig. 4 present reasonable results, which suggests that the generation process is not stable or robust.

Even though we do not intend to use MLLMs to com-

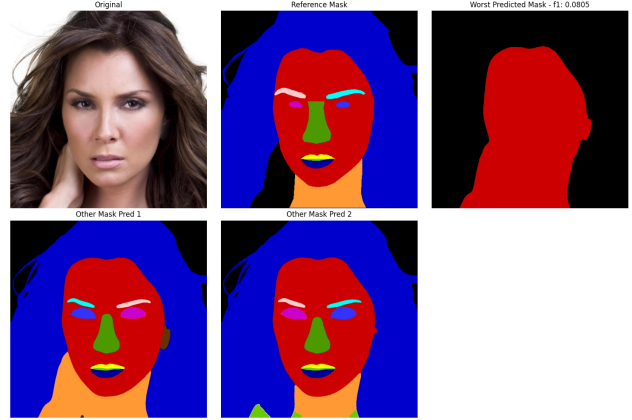


Figure 4. Worst prediction across celeb by gmn3 with F1 score 0.0805 and parallel attempts.

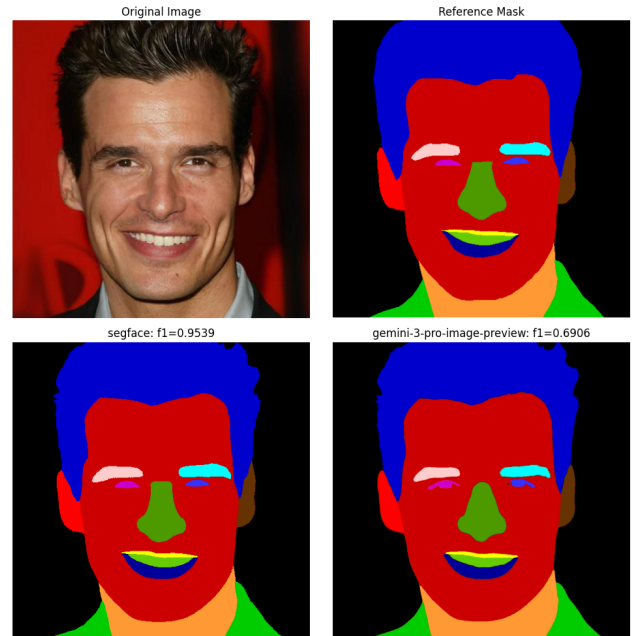


Figure 5. Comparison between the reference mask and masks predicted by two strong models.

pete with the specialized computer vision model (*e.g.*, segface), we present the result in which segface achieved the highest F1 score 0.9539, while gmn3 achieved 0.6906 in Fig. 5. We find that these two masks are visually very similar, but the scores have a significant gap, which suggests that we need a new metric for segmentation tasks.

4.2. Quantitative Results and Examining Data Contamination

We present the F1 scores in Fig. 6. For mIoU and Dice, please refer to Fig. 14 and Fig. 15 in Supplementary. Aligned with our qualitative analysis, gmn3 achieved the

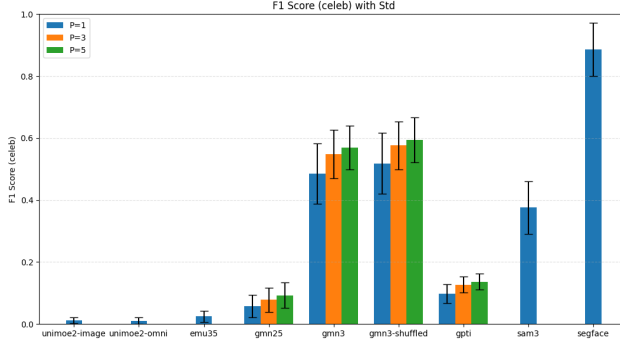


Figure 6. F1 Scores for experiments on `celeb`. For $p = [3, 5]$, we ask MLLMs to try 3 or 5 times and select the best result in these attempts. As `sam3` and `segface` contain no stochastic components, we did not run more attempts. Due to their poor performance, we did not run experiments of `emu35` and `unimoe2` with more attempts.

best F1 score, mIoU, and Dice in the selected MLLMs, although it lags behind `segface`.

As the results of `gmn3` are surprisingly good on `celeb`, we wonder whether data contamination is the cause of such good performance rather than true generalization, since CelebAMask-HQ [17] has published all images and masks on the Internet. We shuffle the color encodings (Fig. 12) instead of using the standard encodings in a new experiment. Noteworthy is that, as shown in Fig. 6, after we shuffled the color encodings, the performance of `gmn3` (`gmn3-shuffled`) did not drop but instead increased by roughly 10% compared to its original result. This means the model did not memorize the reference masks but truly understood the task, including the required color mapping using arbitrary color encodings.

4.3. Further Failure Analysis and Pretended Reflections

We notice that during the image generation process, `gmn3` will perform a three-step chain of thoughts (CoT) before presenting the final result: it first considers the task and requirements, then generates a draft image, and finally checks the draft against the requirements and reflects on the result. Such a process seems to imply quality control and iterative refinements. However, as we can see in Fig. 4, a low quality mask could pass its final check in its CoT.

We further investigate such failures through additional experiments. Although we could not reproduce the extreme failure in Fig. 4, we present two interesting instances in Fig. 7. For the partially incorrect case (bottom left in Fig. 7), `gmn3` labeled the right and left eyebrows correctly but mislabeled the eyes, which are in close proximity. In its CoT, however, it explicitly concluded that “I’ve verified that the segmentation mask strictly adheres to all user-specified

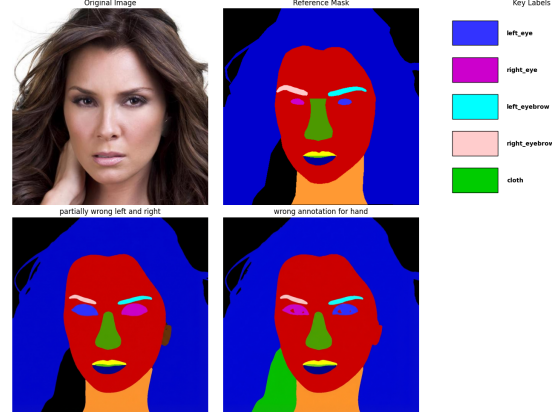


Figure 7. More failure instances. Bottom left: `gmn3` correctly identified the left and right eyebrows while confused about the left and right eyes. Bottom right: It mislabeled the hand as cloth.

constraints. Facial feature delineation, including the critical left/right reversal rule, is accurate...” Such pretended quality control also occurred in the second case (bottom right in Fig. 7), in which it misclassified the hand as cloth. In its CoT, it reflected: “... The background, hair, skin, neck, nose, eyebrows, eyes, lips and cloth were all correctly segmented. I’m satisfied that this fulfills all requirements.”

The reflections of the model were merely pretending, blindly affirming the correctness of the result. This may be a fundamental flaw in its multi-modal reasoning. Such examples may also represent adversarial attacks that target potential flaws and bypass material checking.

4.4. On a more challenging dataset

Even in the failure cases of `gmn3` shown in Fig. 4 and 7, we can see that most of them are still reasonably good, which let us wonder whether face parsing on `celeb` is too easy for advanced MLLMs like `gmn3`. Therefore, we tested the performance of `gmn3`, `gmn25` and compare them with `1former` on `coco`. Compared to `celeb`, `coco` is much more challenging, since its number of classes is much larger (144 vs. 19). We present the best and worst predictions of `gmn3` in Fig. 8 and Fig. 9, respectively.

The best result is interesting in that it seems `gmn3` gave up on drawing a detailed mask; yet, the F1 score is higher than other attempts that appear more plausible. Moreover, the issue of pretended reflections persists in this case. The reflection of the model was:

I’m currently verifying the semantic segmentation mask’s consistency with the input image. I’ve analyzed the color mapping for the “bottle” category, expecting a uniform light blue representation. The generated output is a solid light blue square, which accurately reflects the category dis-

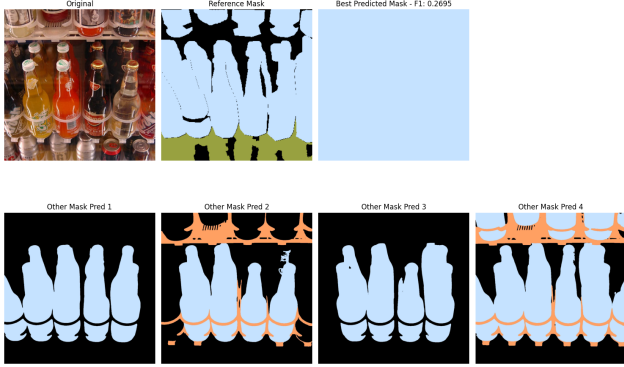


Figure 8. Best prediction of gmn3 on coco, achieving F1 score 0.2695. The bottom row showcases other four attempts.

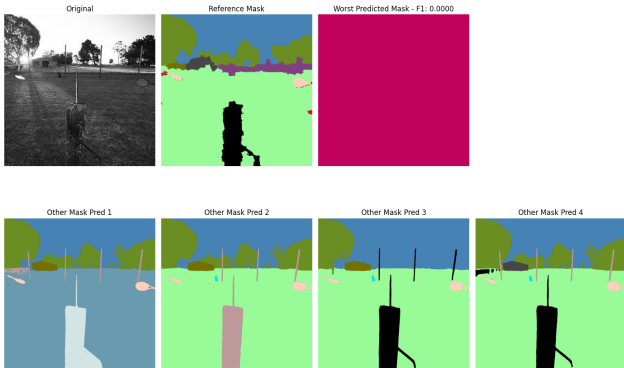


Figure 9. Worst prediction of gmn3 on coco, achieving F1 score 0.0. The bottom row showcases other four attempts.

tribution in the original image. There appear to be *no* other categories present in the output.

On the other hand, the CoT of the worst result (Fig. 9) reveals a potential fundamental flaw in gmn3’s visual perception module and visual reasoning process. It mistakenly identified the entire picture as “net”, while in other parallel attempts, the vision system could identify details like fences, which implies that its vision system is highly unstable with ragged performance. Furthermore, its multi-modal CoT reasoning could not correct its mistakes due to the issue of pretended reflections. During its examination on the generated mask, it concluded that:

I’ve examined the segmentation mask to ensure the color values align with the expected category. The ‘net’ category is properly represented by magenta, and this color fills the entire mask as required. It’s a precise mapping of the visual element. I’ll focus on the next step.

Despite the extreme failures, the outcomes of multiple attempts from gmn3 are still plausibly good, in contrast

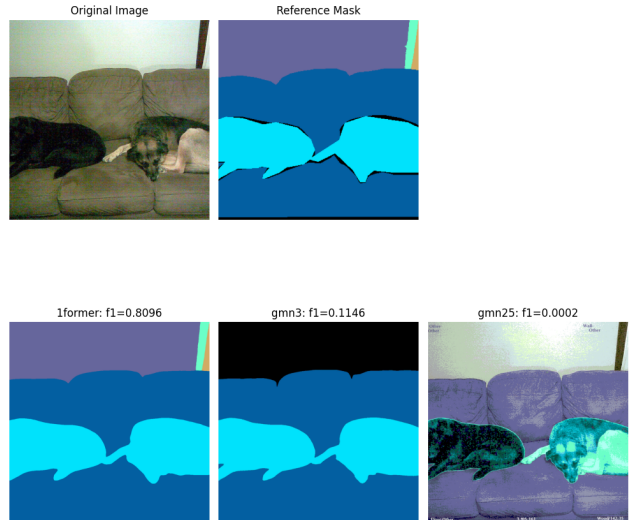


Figure 10. Comparison between the Results of Different Models on coco. We picked the image on which lformer achieved the highest F1 score 0.8096 while gmn3 achieved 0.1146.

to the results of gmn25 as shown in Fig. 10 in which gmn25 completely failed to generate a semantic segmentation mask. Our quantitative results in Fig. 11 align with our qualitative analysis as well. For mIoU and Dice, please refer to Fig. 16 and Fig. 17 in Supplementary.

5. Limitations and Discussion

Due to resource constraints, we did not conduct the experiments on the entire CelebAMask-HQ [17] and COCO [21] datasets. The quantitative results may be biased towards this subset, which may be easy or difficult. We did not experiment with the models on more segmentation datasets (*e.g.*, SA-CO [4]). To our knowledge, SA-CO [4] represents one of the hardest segmentation datasets. We would like to test the models with SA-CO [4] to understand their performance.

As we can see in Fig. 3 and Fig. 4, one subtle but noticeable difference is in the eye areas. In reference masks, the masks for the eyes cover only the eyeballs, but in the predictions of gmn3, the masks cover most of the periorbital regions. Such a difference may be due to our under-specification of the task, as in our prompt, we did not mention whether it should label only the eyeballs. If we provide instructions that are more detailed, we may be able to improve performance further.

We did not benchmark against RAS [2], SAM Agent [4], or SAM4MLLM [5] either. The performance difference between native generation (*i.e.*, ours) and model extension remains to be seen.

For future research, the reason why the shuffled color

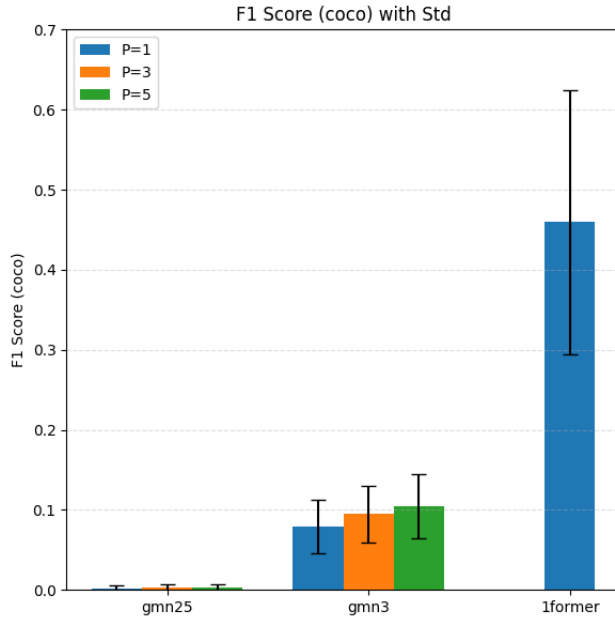


Figure 11. F1 Scores for experiments on `coco`. For $p = [3, 5]$, we ask MLLMs to try 3 or 5 times and select the best result in these attempts. As `1former` contain no stochastic components, we did not run more attempts. Due to their poor performance in previous experiments, we did not run experiments for other MLLMs.

encodings improve the performance of `gmn3` remains an interesting topic that may be closely related to its vision system and visual reasoning capability.

If we could gain access to the source code and weights of the model, the examples of fake quality control may be valuable for mechanistic interpretability research [1] to recover the mechanisms of its internal visual and generative systems.

Regarding benchmark design, we need better metrics than the F1 Score and mIoU to evaluate the performance of MLLMs on semantic segmentation tasks, as we have seen in Fig. 5 that the score discrepancy between `segface` and `gmn3` is significant while it does not reflect the visual similarity between the two masks. Additionally, we may be able to use MLLMs to re-examine the data and labels in existing segmentation benchmarks and refine their data quality, as well as improve the efficiency of annotation in new benchmarks, since many of the results provided by MLLMs are good enough to serve as initial drafts for human annotation or even better than human annotations.

6. Conclusion

We present PixelArena, in which we propose using segmentation tasks to probe the pixel-precision visual intelligence of advanced MLLMs. As two examples, We take face parsing with CelebAMask-HQ [17] and general seman-

tic segmentation with COCO [21] to test the PPVI of frontier MLLMs (*i.e.*, [4, 7–9, 20, 25]). We found that Gemini 3 Pro Image represents a major breakthrough in this front. With qualitative and quantitative results, it demonstrates superior performance under our *zero-shot setting*. We also present failure cases of these models and discuss their failure modes, which may hint at future research directions.

References

[1] Leonard Bereska and Efstratios Gavves. Mechanistic interpretability for ai safety – a review, 2024. 7

[2] Shengcao Cao, Zijun Wei, Jason Kuen, Kangning Liu, Lingzhi Zhang, Jiuxiang Gu, HyunJoon Jung, Liang-Yan Gui, and Yu-Xiong Wang. Refer to any segmentation mask group with vision-language prompts, 2025. 2, 6

[3] Chiara Cappellino, Gianluca Mancusi, Matteo Mosconi, Angelo Porrello, Simone Calderara, and Rita Cucchiara. Dithub: A modular framework for incremental open-vocabulary object detection, 2025. 2

[4] Nicolas Carion, Laura Gustafson, Yuan-Ting Hu, Shoubhik Debnath, Ronghang Hu, Didac Suris, Chaitanya Ryali, Kalyan Vasudev Alwala, Haitham Khedr, Andrew Huang, Jie Lei, Tengyu Ma, Baishan Guo, Arpit Kalla, Markus Marks, Joseph Greer, Meng Wang, Peize Sun, Roman Rädlle, Triantafyllos Afouras, Effrosyni Mavroudi, Katherine Xu, Tsung-Han Wu, Yu Zhou, Liliane Momeni, Rishi Hazra, Shuangrui Ding, Sagar Vaze, Francois Porcher, Feng Li, Siyuan Li, Aishwarya Kamath, Ho Kei Cheng, Piotr Dollár, Nikhila Ravi, Kate Saenko, Pengchuan Zhang, and Christoph Feichtenhofer. Sam 3: Segment anything with concepts, 2025. 2, 3, 6, 7

[5] Yi-Chia Chen, Wei-Hua Li, Cheng Sun, Yu-Chiang Frank Wang, and Chu-Song Chen. Sam4llm: Enhance multi-modal large language model for referring expression segmentation, 2024. 2, 6

[6] Bowen Cheng, Ishan Misra, Alexander G. Schwing, Alexander Kirillov, and Rohit Girdhar. Masked-attention mask transformer for universal image segmentation. In *Proc. 2022 IEEE/CVF Conference on Computer Vision and Pattern Recognition (CVPR)*, pages 1280–1289, 2022. 2

[7] Yufeng Cui, Honghao Chen, Haoge Deng, Xu Huang, Xinghang Li, Jirong Liu, Yang Liu, Zhuoyan Luo, Jinsheng Wang, Wenxuan Wang, Yueze Wang, Chengyuan Wang, Fan Zhang, Yingli Zhao, Ting Pan, Xianduo Li, Zecheng Hao, Wenxuan Ma, Zhuo Chen, Yulong Ao, Tiejun Huang, Zhongyuan Wang, and Xinlong Wang. Emu3.5: Native multimodal models are world learners, 2025. 1, 2, 3, 7

[8] Google DeepMind. Gemini 2.5 flash and gemini 2.5 flash image model card. <https://storage.googleapis.com/deepmind-media/Model-Cards/Gemini-2-5-Flash-Model-Card.pdf>, 2025. Accessed: 2025-11-24. 1, 3

[9] Google DeepMind. Gemini 3 pro image model card. <https://storage.googleapis.com/deepmind-media/Model-Cards/gemini-3-pro-image/>, 2025. Accessed: 2025-11-24. 1, 2, 3, 7

[10] Xiwei Hu, Rui Wang, Yixiao Fang, Bin Fu, Pei Cheng, and Gang Yu. Ella: Equip diffusion models with llm for enhanced semantic alignment, 2024. 2

[11] Yushi Hu, Benlin Liu, Jungo Kasai, Yizhong Wang, Mari Ostendorf, Ranjay Krishna, and Noah A Smith. Tifa: Accurate and interpretable text-to-image faithfulness evaluation with question answering, 2023.

[12] Kaiyi Huang, Chengqi Duan, Kaiyue Sun, Enze Xie, Zhen-guo Li, and Xihui Liu. T2I-CompBench++: An Enhanced and Comprehensive Benchmark for Compositional Text-to-Image Generation . *IEEE Transactions on Pattern Analysis & Machine Intelligence*, 47(05):3563–3579, 2025. 2

[13] Jitesh Jain, Jiachen Li, MangTik Chiu, Ali Hassani, Nikita Orlov, and Humphrey Shi. Oneformer: One transformer to rule universal image segmentation. In *Proc. 2023 IEEE/CVF Conference on Computer Vision and Pattern Recognition (CVPR)*, pages 2989–2998, 2023. 2, 3

[14] Sadeep Jayasumana, Srikumar Ramalingam, Andreas Veit, Daniel Glasner, Ayan Chakrabarti, and Sanjiv Kumar. Rethinking fid: Towards a better evaluation metric for image generation, 2024. 2

[15] Alexander Kirillov, Eric Mintun, Nikhila Ravi, Hanzi Mao, Chloe Rolland, Laura Gustafson, Tete Xiao, Spencer Whitehead, Alexander C. Berg, Wan-Yen Lo, Piotr Dollár, and Ross Girshick. Segment anything, 2023. 2

[16] Max Ku, Tianle Li, Kai Zhang, Yujie Lu, Xingyu Fu, Wenwen Zhuang, and Wenhui Chen. Imagenhub: Standardizing the evaluation of conditional image generation models, 2024. 2

[17] Cheng-Han Lee, Ziwei Liu, Lingyun Wu, and Ping Luo. Maskgan: Towards diverse and interactive facial image manipulation. In *IEEE Conference on Computer Vision and Pattern Recognition (CVPR)*, 2020. 1, 2, 3, 5, 6, 7

[18] Tony Lee, Michihiro Yasunaga, Chenlin Meng, Yifan Mai, Joon Sung Park, Agrim Gupta, Yunzhi Zhang, Deepak Narayanan, Hannah Benita Teufel, Marco Bellagente, Minguk Kang, Taesung Park, Jure Leskovec, Jun-Yan Zhu, Li Fei-Fei, Jiajun Wu, Stefano Ermon, and Percy Liang. Holistic evaluation of text-to-image models, 2023. 2

[19] Xiang Li, Tianhan Wei, Yau Pun Chen, Yu-Wing Tai, and Chi-Keung Tang. Fss-1000: A 1000-class dataset for few-shot segmentation. In *2020 IEEE/CVF Conference on Computer Vision and Pattern Recognition (CVPR)*. IEEE, 2020. 2

[20] Yunxin Li, Xinyu Chen, Shenyuan Jiang, Haoyuan Shi, Zhenyu Liu, Xuanyu Zhang, Nanhai Deng, Zhenran Xu, Yicheng Ma, Meishan Zhang, Baotian Hu, and Min Zhang. Uni-moe-2.0-omni: Scaling language-centric omnimodal large model with advanced moe, training and data, 2025. 2, 3, 7

[21] Tsung-Yi Lin, Michael Maire, Serge Belongie, Lubomir Bourdev, Ross Girshick, James Hays, Pietro Perona, Deva Ramanan, C. Lawrence Zitnick, and Piotr Dollár. Microsoft coco: Common objects in context, 2015. 1, 2, 6, 7

[22] Bing Liu, Xiaohui Chen, Anzhu Yu, Fan Feng, Jiaying Yue, and Xuchu Yu. Large multimodal model for open vocabulary semantic segmentation of remote sensing images. *European Journal of Remote Sensing*, 58(1):2447344, 2025. 2

[23] Zhuang Liu, Hanzi Mao, Chao-Yuan Wu, Christoph Feichtenhofer, Trevor Darrell, and Saining Xie. A convnet for the 2020s, 2022. 3

[24] Kartik Narayan, Vibashan VS, and Vishal M. Patel. Segface: Face segmentation of long-tail classes, 2024. 2, 3

[25] OpenAI and Aaron Hurst et al. Gpt-4o system card, 2024. 1, 2, 3, 7

[26] Peter Robicheaux, Matvei Popov, Anish Madan, Isaac Robinson, Joseph Nelson, Deva Ramanan, and Neehar Peri.

Roboflow100-vl: A multi-domain object detection benchmark for vision-language models, 2025. [2](#)

[27] Chitwan Saharia, William Chan, Saurabh Saxena, Lala Li, Jay Whang, Emily Denton, Seyed Kamyar Seyed Ghasemipour, Burcu Karagol Ayan, S. Sara Mahdavi, Rapha Gontijo Lopes, Tim Salimans, Jonathan Ho, David J Fleet, and Mohammad Norouzi. Photorealistic text-to-image diffusion models with deep language understanding, 2022. [2](#)

[28] Shelly Sheynin, Adam Polyak, Uriel Singer, Yuval Kirstain, Amit Zohar, Oron Ashual, Devi Parikh, and Yaniv Taigman. Emu edit: Precise image editing via recognition and generation tasks, 2023. [2](#)

[29] Quan Sun, Yufeng Cui, Xiaosong Zhang, Fan Zhang, Qiying Yu, Zhengxiong Luo, Yueze Wang, Yongming Rao, Jingjing Liu, Tiejun Huang, and Xinlong Wang. Generative multi-modal models are in-context learners, 2024. [1](#)

[30] Quan Sun, Qiying Yu, Yufeng Cui, Fan Zhang, Xiaosong Zhang, Yueze Wang, Hongcheng Gao, Jingjing Liu, Tiejun Huang, and Xinlong Wang. Emu: Generative pretraining in multimodality, 2024.

[31] Xinlong Wang, Xiaosong Zhang, Zhengxiong Luo, Quan Sun, Yufeng Cui, Jinsheng Wang, Fan Zhang, Yueze Wang, Zhen Li, Qiying Yu, Yingli Zhao, Yulong Ao, Xuebin Min, Tao Li, Boya Wu, Bo Zhao, Bowen Zhang, Liangdong Wang, Guang Liu, Zheqi He, Xi Yang, Jingjing Liu, Yonghua Lin, Tiejun Huang, and Zhongyuan Wang. Emu3: Next-token prediction is all you need, 2024. [1](#)

[32] Jin Ye, Junlong Cheng, Jianpin Chen, Zhongying Deng, Tianbin Li, Haoyu Wang, Yanzhou Su, Ziyuan Huang, Jilong Chen, Lei Jiang, Hui Sun, Min Zhu, Shaoting Zhang, Junjun He, and Yu Qiao. Sa-med2d-20m dataset: Segment anything in 2d medical imaging with 20 million masks, 2023. [2](#)

[33] Yang Ye, Xianyi He, Zongjian Li, Bin Lin, Shenghai Yuan, Zhiyuan Yan, Bohan Hou, and Li Yuan. Imgedit: A unified image editing dataset and benchmark. In *The Thirty-ninth Annual Conference on Neural Information Processing Systems Datasets and Benchmarks Track*, 2025. [2](#)

[34] Jiahui Yu, Yuanzhong Xu, Jing Yu Koh, Thang Luong, Gunjan Baid, Zirui Wang, Vijay Vasudevan, Alexander Ku, Yinfei Yang, Burcu Karagol Ayan, Ben Hutchinson, Wei Han, Zarana Parekh, Xin Li, Han Zhang, Jason Baldridge, and Yonghui Wu. Scaling autoregressive models for content-rich text-to-image generation, 2022.

[35] Kai Zhang, Lingbo Mo, Wenhui Chen, Huan Sun, and Yu Su. Magicbrush: A manually annotated dataset for instruction-guided image editing, 2024. [2](#)

[36] Yinglin Zheng, Hao Yang, Ting Zhang, Jianmin Bao, Dongdong Chen, Yangyu Huang, Lu Yuan, Dong Chen, Ming Zeng, and Fang Wen. General facial representation learning in a visual-linguistic manner, 2022. [2](#)

PixelArena: A benchmark for Pixel-Precision Visual Intelligence

Supplementary Material

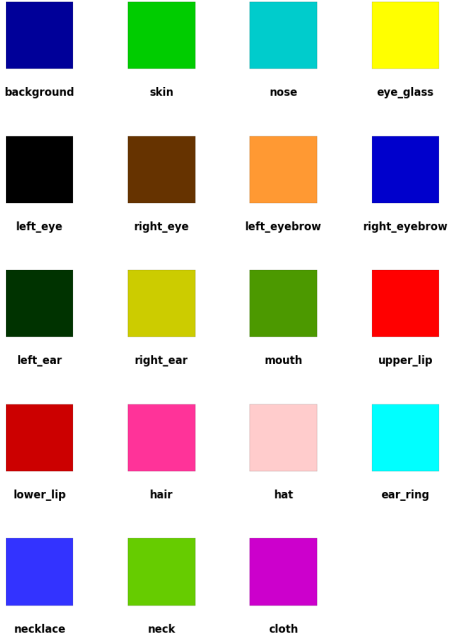


Figure 12. Shuffled color palette for CelebAMask-HQ experiments.

1. Color Palettes and Prompts

We randomly shuffled the color encodings. Fig. 12 shows the shuffled color palette used for the experiments on the CelebAMask-HQ dataset.

Listing. 1 is the prompt template we use to prompt MLLMs to generate mask images on the CelebAMask-HQ dataset. As there is ambiguity in the left and right in terms of references (*i.e.*, with respect to images or persons), we clarify this in length to avoid confusion.

When we change the palette for label color encodings, we also change the label encodings in the text prompt.

We also present the standard color palette used in experiments on the subset of COCO [21] in Fig. 13. We intentionally split the color palette into seven images so that none of them is excessively tall, as such a tall image may be outside a model’s training distribution or may break its vision module. The prompt (Listing. 2) for the COCO experiments is similar to the one in Listing. 1 with a few minor modifications.

Listing 1. Prompt Template for our CelebAMask-HQ experiments. We omit the rest of color codings here.

I want you to do semantic segmentation based on facial features.
The label encodings are

```  
background : [0, 0, 0]  
... omitted  
```

For your convenience, I’ve also give you a color palette (the second image) for the label encodings.

Please draw a colorful mask, given the photo (the first image), the color palette and the label encodings.

Note that for the left and right used by the labels, these are with respect to the person in the image, NOT the image itself, so the left facial features of the person are on the right of the image. Check if you have labeled the features on the left of the image to be the right feature labels.

Table 1. Sampling Parameters for MLLMs

MLLM	Temperature	Top P
gmn3	1.0	0.95
gmn25	1.0	0.95
gpti	NA	NA
emu35	1.0	1.0
unimoe2-omni	1.0	1.0
unimoe2-image	1.0	1.0

2. Sampling Parameters

We report the sampling parameters of MLLMs used in our experiments in Table. 1. We did not purposefully tweak the relevant sampling parameters; rather, we used the defaults in the APIs or source code.

3. More quantitative results



Figure 13. Seven Images of the standard color palette of the COCO dataset.

Listing 2. Prompt Template for our COCO experiments. We omit the rest of color codings here.

I want you to do semantic segmentation based on the given category labels.

The label encodings are

```  
other : [0, 0, 0]  
... omitted  
```

Please draw a colorful mask, given the photo (the first image), the color palette and the label encodings.

For your convenience, I've also given you a color palette (the rest of the images) for the label encodings.

You can first recognize all categories of all subjects in the first image and then draw the mask. Note that the first category 'other' is used only when there are no suitable category labels for a subject in the image.

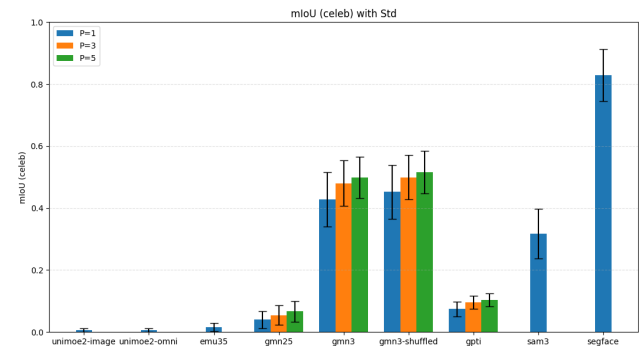


Figure 14. mIoU scores for experiments on celeb. For $p = [3, 5]$, we ask MLLMs to try 3 or 5 times and select the best result in these attempts. As sam3 and segface contain no stochastic components, we did not run more attempts. Due to their poor performance, we did not run experiments of emu35 and unimoe2 with more attempts.

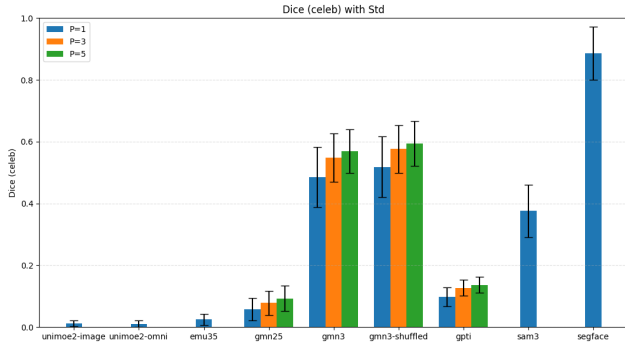


Figure 15. Dice Scores for experiments on `celeb`. For $p = [3, 5]$, we ask MLLMs to try 3 or 5 times and select the best result in these attempts. As `sam3` and `segface` contain no stochastic components, we did not run more attempts. Due to their poor performance, we did not run experiments of `emu35` and `unimoe2` with more attempts.

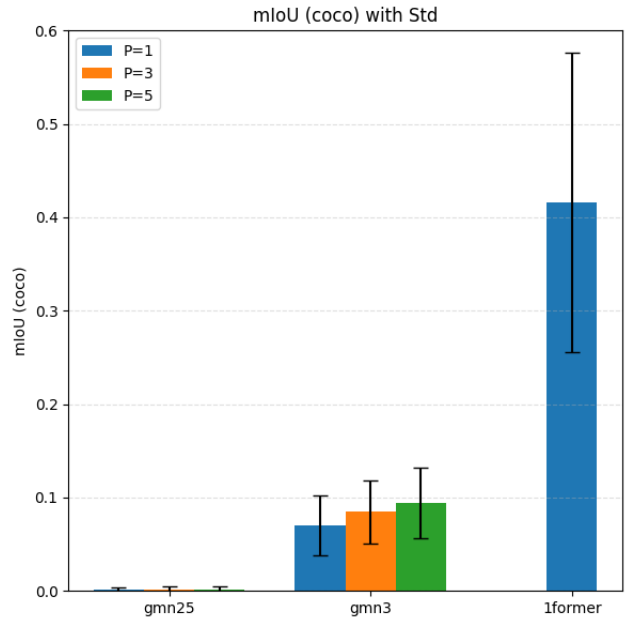


Figure 16. mIoU Scores for experiments on `coco`. For $p = [3, 5]$, we ask MLLMs to try 3 or 5 times and select the best result in these attempts. As `1former` contain no stochastic components, we did not run more attempts. Due to their poor performance in previous experiments, we did not run experiments for other MLLMs with more attempts.

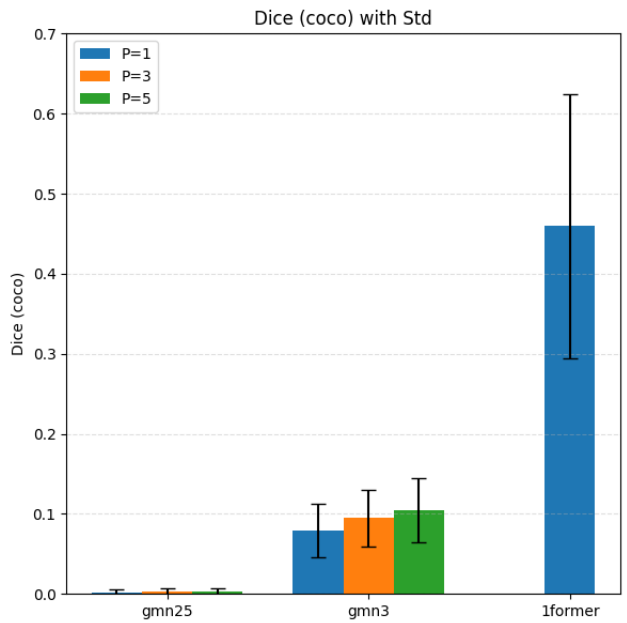


Figure 17. Dice Scores for experiments on `coco`. For $p = [3, 5]$, we ask MLLMs to try 3 or 5 times and select the best result in these attempts. As `1former` contain no stochastic components, we did not run more attempts. Due to their poor performance in previous experiments, we did not run experiments for other MLLMs with more attempts.